Annals of Nuclear Medicine Vol. 4, No. 1, 1–13, 1990

# Differentiation of bronchogenic carcinoma from secondary changes, obstructive pneumonitis and/or collapse by I-123 IMP lung imaging

Masayuki NAKAJO*, Noriaki UCHIYAMA*, Jurio SHIMADA*, Shinji SHINOHARA*, Atsushi IRIKI**, Yasunobu HIROTSU**, Katsushi EGAWA**, Hidetomo FUKUNAGA** and Yoshimasa NORIMATSU**

*Department of Radiology, Faculty of Medicine, Kagoshima University
**Departments of Respiratory Surgery and Internal Medicine, Minami-Kyushu Hospital, Kagoshima, Japan

Serial lung images with N-isopropyl-p-[I-123]-iodoamphetamine (I-123 IMP) were obtained to assess the imaging findings and to clarify the lesion to uptake relationships in 74 lesions in 73 patients with various histological types of bronchogenic carcinoma. A decreased uptake area was observed in all 74 lesions in the initial one or two-min I-123 IMP image. The initial image was analogous to a Tc-99m MAA lung perfusion image in 70 patients in whom both lung imaging procedures were performed. The imaging findings changed following this initial phase. At 4 hr, the lesion was depicted as either areas of decreased uptake or increased uptake or a combination of the two. Comparison between the lesion findings in the 4-hr I-123 IMP images, radiograms and removed specimens revealed that areas of decreased uptake corresponded to the cancerous portions of the lung mass or pleural effusion and areas of increased uptake corresponded to inflammatory portions including obstructive pneumonitis and/or collapse. Thus, the 4-hr I-123 IMP lung images can be used to discriminate the cancerous portion from associated secondary changes, obstructive pneumonitis and/or collapse.

**Key words:** I-123 IMP, lung imaging, bronchogenic carcinoma, lung collapse, obstructive pneumonitis

## INTRODUCTION

N-isopropyl-p-[I-123]iodoamphetamine (I-123 IMP), which was originally developed as a brain perfusion imaging agent,[1] has been shown to be a potential agent for nonparticulate lung perfusion and metabolic lung imaging.[2] An incidental finding was that a focal uptake of I-123 IMP was related to a patient's bronchogenic carcinoma.[3] This suggested that I-123 IMP might show different accumulation in different pathological conditions of the lung. Therefore, we performed serial lung imaging with I-123 IMP in patients with bronchogenic carcinoma to clarify the relationships of lesion to uptake of activity.

Received August 23, 1989, revision accepted November 30, 1989.

For reprints contact: M. Nakajo, Department of Radiology, Faculty of Medicine, Kagoshima University, 1208–1 Usuki-cho, Kagoshima-shi, Kagoshima 890, JAPAN.

We report here that I-123 IMP accumulated gradually in the obstructive pneumonitis and/or collapse secondary to the lung cancer which itself showed an impaired uptake of I-123 IMP. Thus 4-hr I-123 IMP lung imaging can be used to discriminate between the cancerous portion and secondary changes, obstructive pneumonitis and/or collapse in patients with bronchogenic carcinoma.

## MATERIALS AND METHODS

Study population: From Aug., 1986 to Mar., 1988, a total of 87 patients suspected of having bronchogenic carcinoma were referred for I-123 IMP lung and brain scintigraphy. Of these, 73 patients were histologically confirmed to have bronchogenic carcinoma and had radiographic evidence of a pulmonary lesion. The histological diagnosis was made from the specimen obtained by fiberoptic bronchoscopy or operation. These 73 patients were included

in this study; 39 with squamous cell carcinoma (SqCC), 17 with adenocarcinoma (Adenoca), 12 with small cell carcinoma (SCLC), 2 with large cell carcinoma (LCC) and 3 with bronchiolo-alveolar carcinoma (BAC). There were 59 males and 14 females, with an age range of 32 to 85 yr at the time of imaging.

Imaging methods: Thyroidal uptake of free I-123 was blocked by oral administration of potassium iodide 100 mg×3 a day, beginning on the day before i.v. injection of I-123 IMP (Nihon Mediphysics, Japan) and continuing for 3 days afterwards. Anterior or posterior dynamic lung imaging was acquired for 25 mins with one frame/min immediately after i.v. injection of 111 MBq (3 mCi) in a volume of 3 m*l* using a medium energy multiparallel hole collimator attached to a gamma camera. The patient was positioned supine or prone so that the lesion was closest to the surface of the collimator. Thirty-min and 4-hr static images were also obtained from six projections: anterior, posterior, bilateral and both anterior or posterior 45° oblique views. Selection of the oblique projections was determined by anterior or posterior location of the lesion in the chest X-ray lateral view. A 20% window was centered on the 159-KeV photopeak and 500,000 counts were acquired for each view. After lung imaging, I-123 brain images were also obtained to examine for the presence or absence of metastatic brain tumor.

Diagnostic methods for comparison: Tc-99m macroaggregated albumin (MAA) lung perfusion imaging was also performed in 70 patients after i.v. injection of 185 MBq (5 mCi) of Tc-99m MAA to identify the lesion and compare the findings in I-123 IMP and Tc-99m MAA imaging. For MAA imaging, 300,000 counts were acquired for each of the same 6 views as obtained in the static I-123 IMP lung imaging. The energy window was 20% centered on the 140 KeV energy emission of Tc-99m. The interval between the two imaging procedures was two days.

Routine chest X-ray PA and lateral films and tomograms were obtained in all patients. In addition, chest X-ray films were obtained from 5 projections (PA or AP, left and right lateral, and both anterior or posterior 45° view) in the same normal respiration and positions as the static IMP images were obtained so that the comparison between the lesion locations could be made precisely on I-123 IMP and Tc-99m MAA images, and radiograms. These X-ray films were obtained on the same day as I-123 IMP imaging was performed in most patients and within one week in the remainder. The other diagnostic procedures included transmission computed tomography (TCT), Ga-67 tumor and Tc-99m MDP bone imaging.

The lung specimen was surgically obtained in 29 patients. The operation was performed within 2 weeks in 22 cases, from 20 to 27 days in 6 cases and at 50 days in one case after I-123 IMP lung imaging. The chest X-ray findings at operation showed no significant changes when compared to those obtained at the time of I-123 IMP imaging. In one patient, a 24-hr I-123 IMP image of the removed left lower lung was also obtained so that direct pathological comparison of the removed specimen and the image of I-123 IMP biodistribution could be made.

Methods of study: First, the serial changes in I-123 IMP imaging findings were examined. Confirmation of the location and extent of the lesion was made by comparing the IMP images with 5 chest X-ray views, 6 Tc-99m MAA views, when available, and chest X-ray tomograms and/or TCT images, if necessary. The pulmonary findings in the initial one-min IMP image and Tc-99m MAA image were also compared. The two-min IMP image was used, when the one-min IMP image was not suitable for comparison due to the activity in the subclavian and brachiocephalic veins, superior vena cava and cardiac cavities. The lesion findings in the IMP images were visually determined by using the uptake in the lung fields near the lesion as a normal uptake.

Next, the lesion findings in the 4-hr I-123 IMP images and chest X-ray films were compared. The lesion findings in the chest X-ray films were divided into a mass shadow only, a mass shadow with secondary shadow(s), secondary shadow(s) only and a diffuse homogenous shadow. The mass shadow meant a demarcated round, oval or lobulated shadow with a measurable diameter. The secondary shadows included infiltrates, consolidation, honeycombing, collapse, metastatic small coin lesions and pleural effusion. Infiltrates meant patchy shadows, clouding or ill-defined opacity which mainly represented alveolar patterns. The diffuse homogeneous shadow meant a large ill-defined homogeneous shadow in which the tumor could not be identified, even by means of chest tomograms. The mass shadow could be identified in a total of 53 lesions in 52 patients. One patient with SqCC had two separate mass shadows. The average diameter of the mass shadow ranged between 3.0 and 8.5 cm in 26 patients with SqCC, 2.5 and 8.0 cm in 14 with Adenoca, 4.0 and 9.8 cm in 9 with SCLC, 3.3 and 8.5 cm in 2 with LCC and was 5.8 cm in one with BAC. The mass shadow only was observed in 16 lesions. The secondary shadow(s) only were observed in 19 lesions. Of these, two with BAC had infiltrates only. The diffuse homogeneous shadow was observed in each one with SqCC and SCLC. The mass shadow with secondary shadow(s) was observed in the 37 other lesions. The findings in IMP images and chest X-ray films were observed and determined by more than two of the authors (a common observer was M.N.).

Comparison of the lesion findings in 4-hr I-123 IMP images and surgically removed specimens was macroscopically performed when tissue sections were done. Before this comparison, we discussed the correlation between the lesion findings on chest X-ray films including tomograms, TCT, I-123 IMP and Tc-99m MAA images. The microscopic examinations were mainly performed in the regions including the cancerous portions and adjacent tissues where the biodistribution of I-123 IMP had changed. If the site of abnormal accumulation was apart from the main tumor, the site was also examined microscopically.

## RESULTS

*Serial changes in I-123 IMP lung imaging findings*

After i.v. injection of I-123 IMP, the activity in the lung fields outside of the lesion was initially high and decreased gradually. This fall was accompanied by a gradual increase with time in the hepatic activity. The findings in the initial one or 2-min dynamic I-123 IMP lung images were analogous to those in Tc-99m MAA lung perfusion images in 70 patients in whom the comparison of these images was possible, and decreased activity was observed in all 71 lesions (note one patient had 2 lesions). The other 3 lesions also showed decreased uptake in the initial dynamic IMP images. However, the I-123 IMP imaging findings subsequently changed. At 30 min, the following I-123 IMP imaging patterns were observed; a decreased uptake area, a decreased uptake area with a normal uptake area, a decreased uptake area with an increased uptake area, a normal uptake area, an increased uptake area, a decreased uptake

**Table 1** Changes from 30 min to 4 hr in I-123 IMP lung lesion patterns

| $^{123}$I-IMP lesion patterns* | | Histological types of bronchogenic cancer** | | | | | Total |
|---|---|---|---|---|---|---|---|
| 30 min | 4 hr | Sqcc | Adenoca | SCLC | LCC | BAC | |
| D | D | | 5 | 1 | 1 | 2 | 9 |
| D+N | D+I | 13 | 4 | 6 | 1 | | 24 |
| D+I | D+I | 3 | 1 | 1 | | 1 | 6 |
| D+I | D+FI | 14 | 3 | 2 | | | 19 |
| D | I | 4 | | | | | 4 |
| N | I | 3 | 1 | 2 | | | 6 |
| I | FI | 2 | 1 | | | | 3 |
| D+I+D | D+FI+D | 1 | 1 | | | | 2 |
| N+D | I+D | | 1 | | | | 1 |
| Total | | 40 | 17 | 12 | 2 | 3 | 74 |

* Abbreviations are as follows: D; a decreased uptake area, N; a normal uptake area, I; an increased uptake area, FI; an area where increased uptake at 30 min increased further at 4 hr, and +; with.

** Sqcc; squamous cell carcinoma, Adenoca; adenocarcinoma, SCLC; small cell carcinoma, LCC; large cell carcinoma and BAC; bronchiolo-alveolar carcinoma.

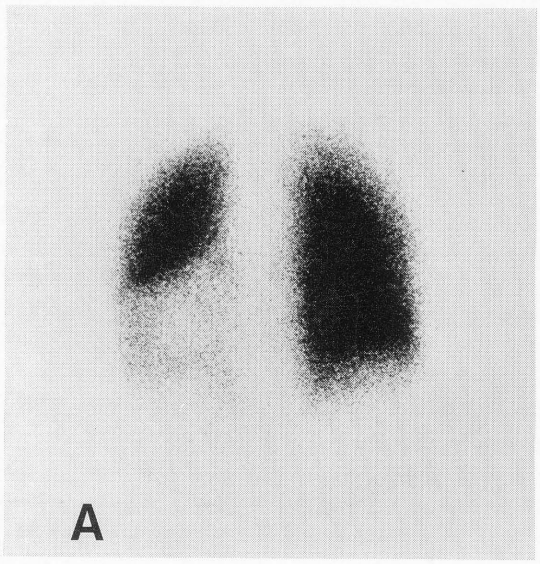


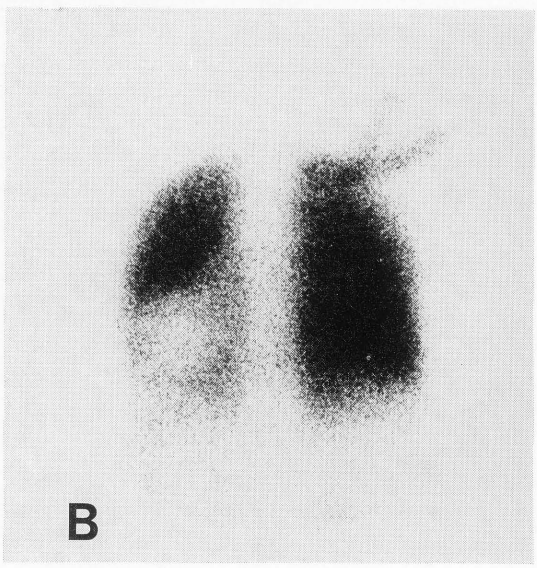

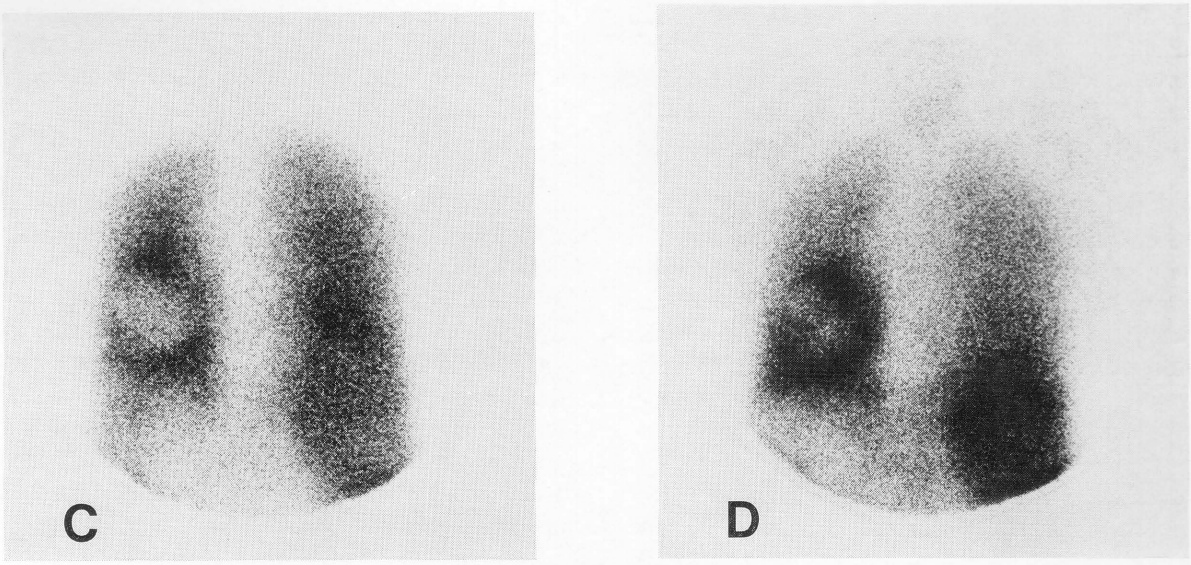


**Fig. 1** An example of Tc-99m MAA lung perfusion image and serial changes in I-123 imaging findings in a 49-yr-old female with SCLC. The perfusion image (A) is analogous to a one-min I-123 IMP image (B). The pattern of a decreased uptake area with an increased uptake area at 30 min (C) changed into the pattern of a decreased uptake area with a further increased uptake area at 4 hr (D).

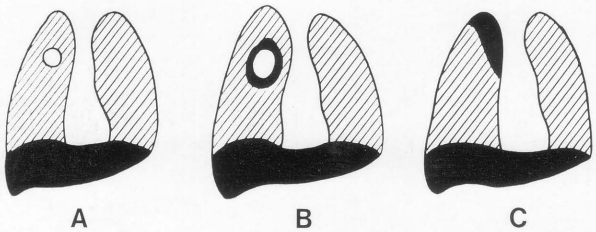


**Fig. 2** The basic lesion patterns in 4-hr I-123 IMP lung images. A: a decreased uptake area, B: a decreased uptake area with an increased or further increased uptake area and C: an increased or further increased uptake area.

area with increased and decreased uptake areas and a normal uptake area with a decreased uptake area. Changes in the lesion imaging patterns between 30 min and 4 hr are shown in Table 1: In general, further decreases in normal activity and increases in activity of all or certain parts of the lesion were observed in the subsequent 4-hr I-123 IMP lung images. The 4-hr IMP lesion patterns were constituted by a decreased uptake area, an increased uptake area and a further increased uptake area (an area where intense activity at 30 min increased further at 4 hr) and a combination of these. In some cases, the decreased uptake area at 4 hr was not so clear as that observed in the 30-min I-123 IMP image due to decreases in activity outside of the lesion.

An example of a Tc-99m MAA lung perfusion image and serial changes in I-123 IMP imaging finding is shown in Fig. 1. In Fig. 2 are schematically shown the basic lesion imaging patterns at 4 hr; a decreased uptake area, a decreased uptake area with an increased or further increased uptake area, and an increased uptake area.

*Comparison of 4-hr I-123 IMP images with chest X-ray films*

Table 2 shows a comparison between lung lesion findings on 4-hr I-123 IMP images and chest X-ray films. The pattern of a decreased uptake was observed in 9 lesions and corresponded to the mass shadow only in 7 of them (Fig. 3). In one patient, this pattern corresponded to the infiltrates only which represented BAC (Fig. 4). The pattern of a decreased uptake area with an increased or further increased uptake area was observed in 49 lesions and corresponded to the mass shadow with secondary shadow(s) in 35 of them (Fig. 5). This pattern also corresponded to the mass shadow only in 8 lesions, the secondary shadow(s) only in 4 lesions (Fig. 6) and the homogeneous shadow in 2 lesions (Fig. 7). The pattern of an increased or further increased uptake area was observed in 13 lesions and corresponded to the secondary shadow(s) only in 12 lesions (Fig. 8). This pattern appeared to correspond to the mass shadow only in one patient (Fig. 9).

To elucidate which radiographic shadows represent the decreased uptake area and the increased or further increased uptake area respectively, further analysis was done (Table 3). There were a total of 63 decreased uptake areas. The area corresponded to a mass shadow in 52 lesions, the whole or greater part of infiltrates later proven to be BAC in 2 lesions, a

**Table 2** Comparison of lung lesion findings in 4-hr $^{123}$I-IMP images and chest X-ray films

| Chest X-ray findings<br>Main shadow+secondary shadow(s) | 4-hr $^{123}$I-IMP lesion patterns* | | | | | | | Total |
|---|---|---|---|---|---|---|---|---|
| | D | D+I | D+FI | I | FI | D+FI+D | I+D | |
| Mass only | 7 | 7 | 1 | 1 | | | | 16 |
| Mass+infiltrates | | 12 | 15 | | | | | 27 |
| Mass+consolidation | | 1 | | | | | | 1 |
| Mass+honeycombing | | 2 | | | | | | 2 |
| Mass+hoheycombing infiltrates | | | 2 | | | | | 2 |
| Mass+collapse | | 3 | | | | | | 3 |
| Mass+metastatic small coin lesions | 1 | | | | | | | 1 |
| Mass+collapse+pleural effusion | | | | | | 1 | | 1 |
| Infiltrates only | 1 | 3 | | 2 | | | | 6 |
| Infiltrates+consolidation | | | | 1 | | | | 1 |
| Collapse only | | 1 | | 6 | 3 | | | 10 |
| Collapse+pleural effusion | | | | | | 1 | 1 | 2 |
| Diffuse homogeneous shadow | | 1 | 1 | | | | | 2 |
| Total | 9 | 30 | 19 | 10 | 3 | 2 | 1 | 74 |

* Abbreviations are the same as used in Table 1.

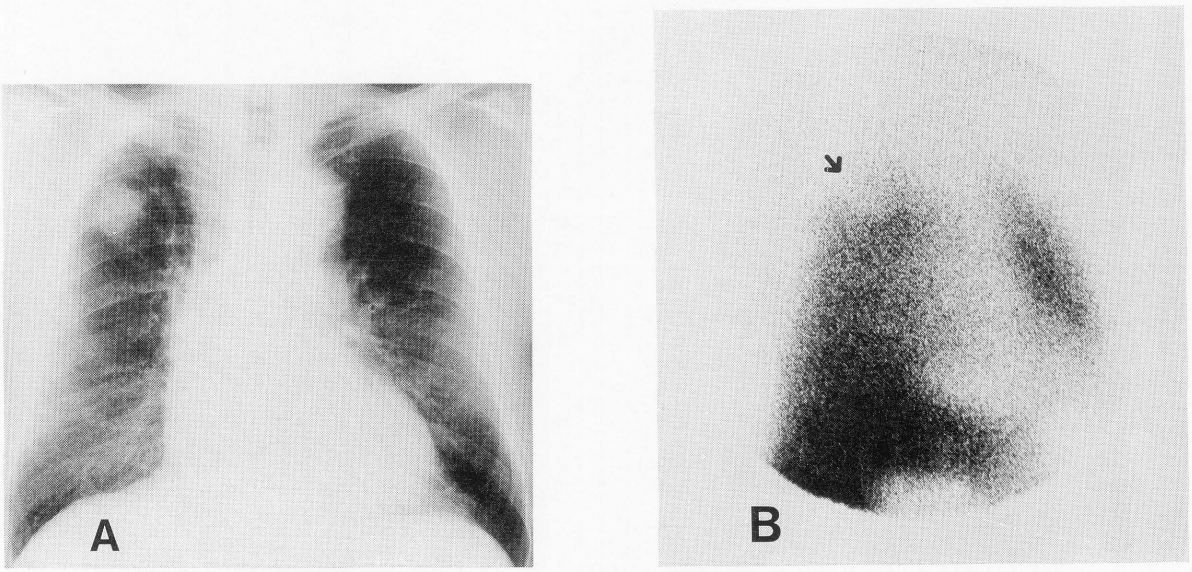


**Fig. 3** A 72-yr-old-man with LCC. The chest radiogram (A) shows a mass shadow only in the right upper lobe which is represented as a decreased uptake area (arrow) in the 4-hr I-123 IMP right anterior oblique view (B).

part of infiltrates, collapse and diffuse homogeneous shadows in 6 lesions, and pleural effusion in 3 lesions. There were a total of 65 increased or further increased uptake areas. The area corresponded to infiltrates with or without consolidation or honeycombing in 35 lesions, collapse in 16 lesions, honeycombing in 2 lesions, consolidation in one lesion, a part of diffuse homogeneous shadow in two lesions and appeared to correspond to a mass shadow in one lesion. In the remaining 8 lesions, the increased or further increased uptake area corresponded to the marginal area surrounding a mass shadow which had no visible changes such as infiltrates or collapse.

To summarize these results, at 4 hr there appeared to be two types of I-123 IMP accumulation in the lung lesions of patients with bronchogenic carcinoma; one type was decreased accumulation of I-123 IMP in cancerous portions and in pleural

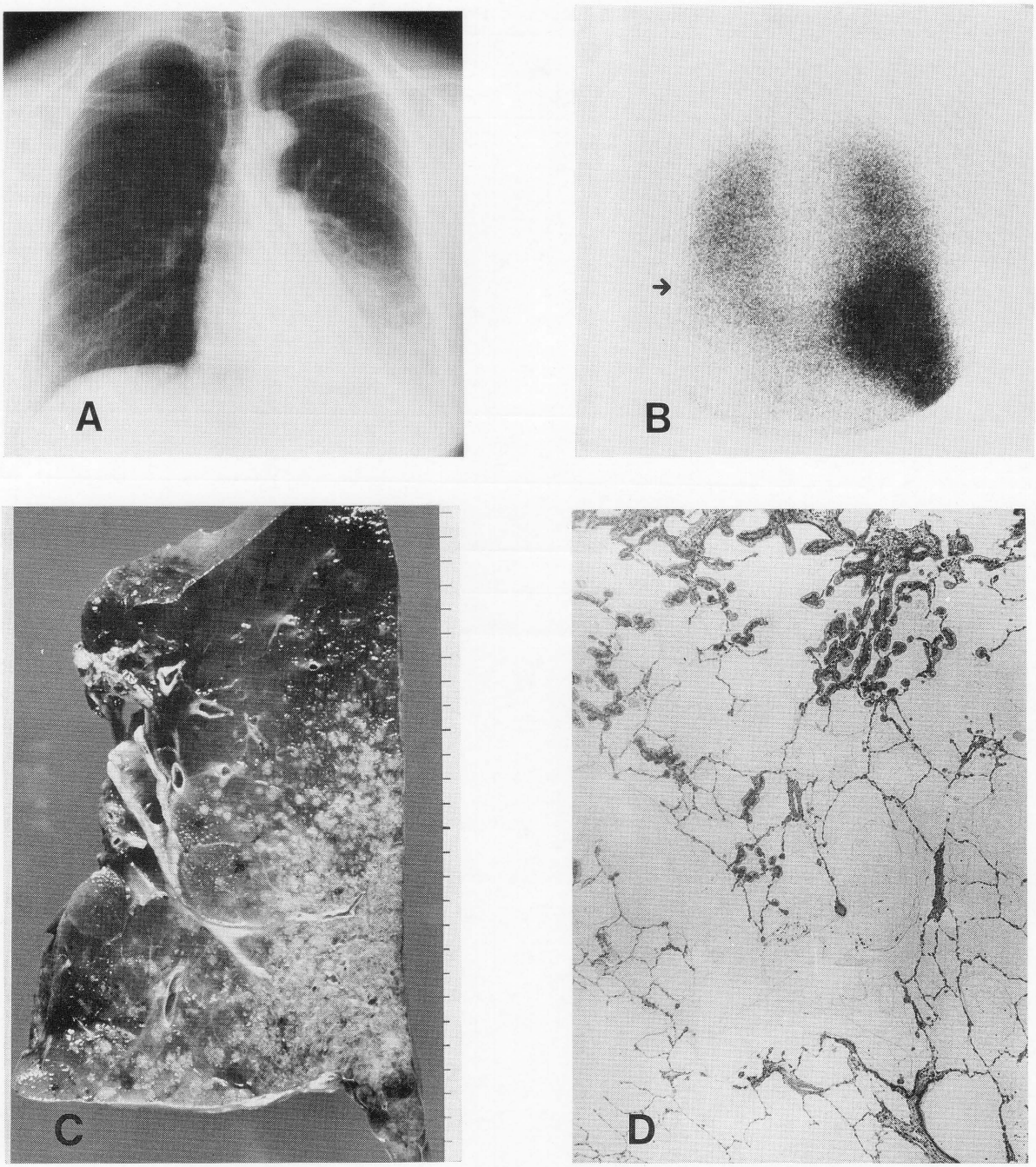


**Fig. 4** A 55-yr-old-female with BAC. The chest radiogram (A) shows infiltrates in the left lower lobe. The lesion is delineated as a decreased uptake area (arrow) in the 4-hr posterior I-123 IMP image (B). The removed left lower lung (C) was replaced by BAC with plentiful mucin in alveoli (D).

effusion and the other was intense accumulation of I-123 IMP in noncancerous infiltrates and consolidation, collapse and honeycombing.

*Comparison of 4-hr I-123 IMP images and removed specimens*

To pathologically confirm the lesion to uptake relationships, the findings on 4-hr I-123 IMP images were compared with those of the removed specimens in 29 patients (Table 4). There were 11 decreased uptake areas in 18 patients with SqCC. All the decreased uptake areas corresponded to the tumors. The remaining 7 tumors were too small to assess the lesion to uptake relationships: Two were intraluminal tumors and 5 were 12 to 25 mm in average diameter. The increased or further increased uptake area corresponded to obstructive pneumonitis, congestion, congestive edema, bronchopneumonia and collapse

or a combination of these in all 18 lesions. Representative cases of SqCC with obstructive pneumonitis and/or collapse are shown in Figs. 6–8. There were 7 decreased uptake areas in 8 patients with Adenoca. All 7 decreased uptake areas corresponded to the tumors. A tumorous shadow represented as an increased uptake area was composed of a tumor, $31 \times 29 \times 30$ mm in size with surrounding obstructive pneumonitis, congestive edema and infarction (Fig. 9). The remaining 4 normal uptake areas surrounding tumors exhibited no significant pathological changes. In a patient with intraluminal SCLC, an increased uptake area corresponded to obstructive pneumonitis and congestive edema. In two patients with BAC which showed infiltrates in the chest X-ray films, the tumor was represented as a decreased uptake area (Fig. 4). An increased uptake area corresponded to interstitial pneumonia with granuloma in a patient with BAC.

These results further confirmed that the decreased uptake areas corresponded to the cancerous portions and the increased or further increased uptake areas represented noncancerous lesions such as obstructive pneumonitis and collapse.

## DISCUSSION

Whole body biodistribution studies in humans revealed that I-123 IMP uptake was seen in lung, liver and brain.[3] The utility of this agent in brain studies has been shown in the assessment of pathological states related to abnormal cerebral blood flow.[3–7]

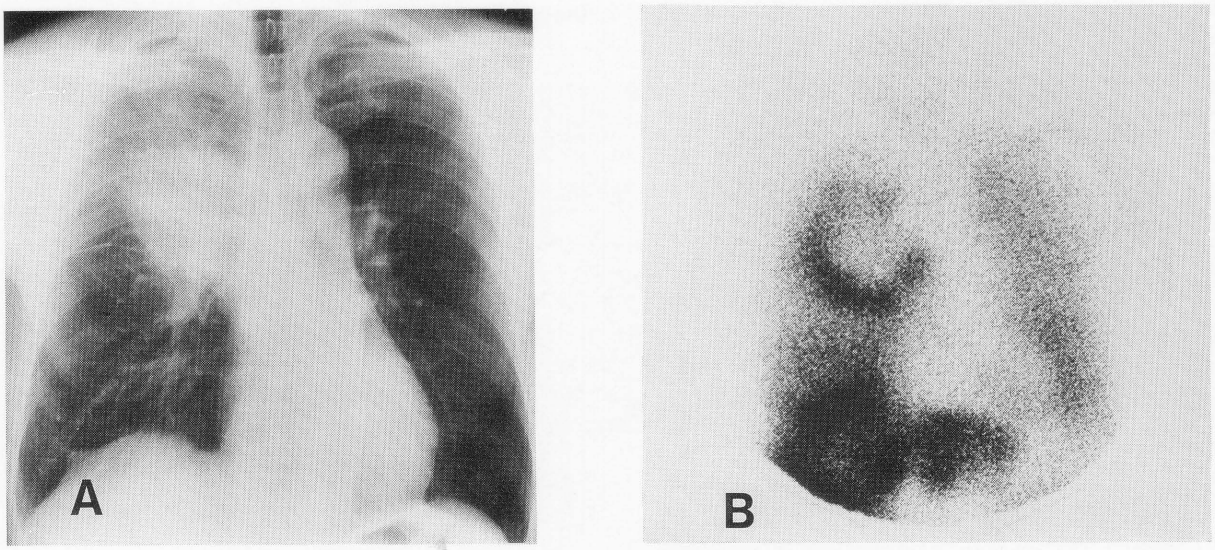


**Fig. 5** A 70-yr-old man with SqCC. The chest radiogram (A) shows a mass shadow surrounded by infiltrates. The 4-hr I-123 IMP image shows a decreased uptake area with a further increased uptake area (B).

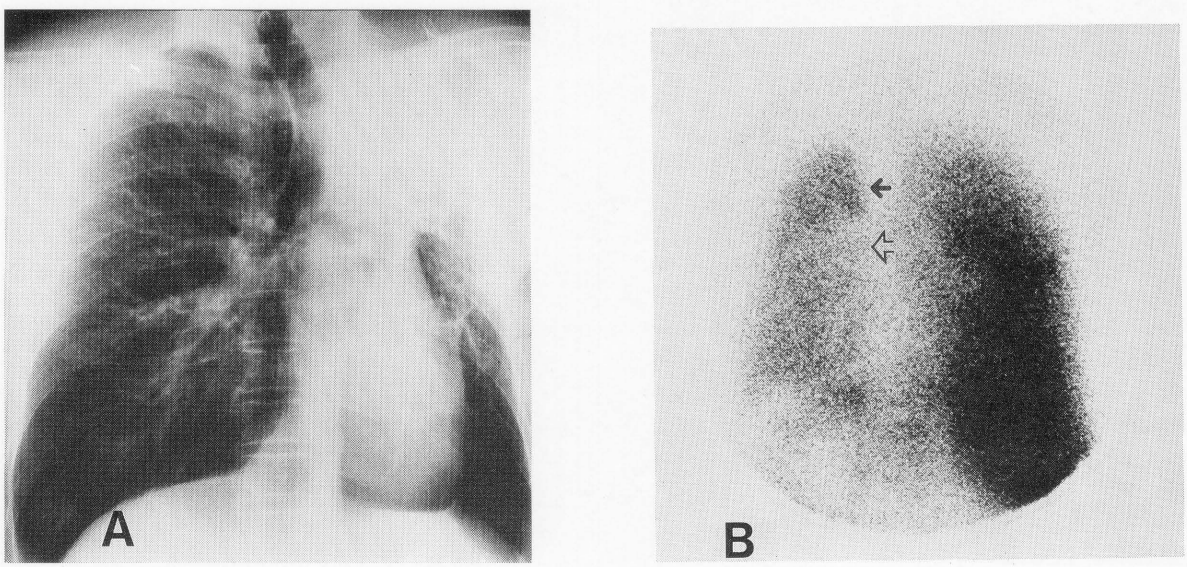

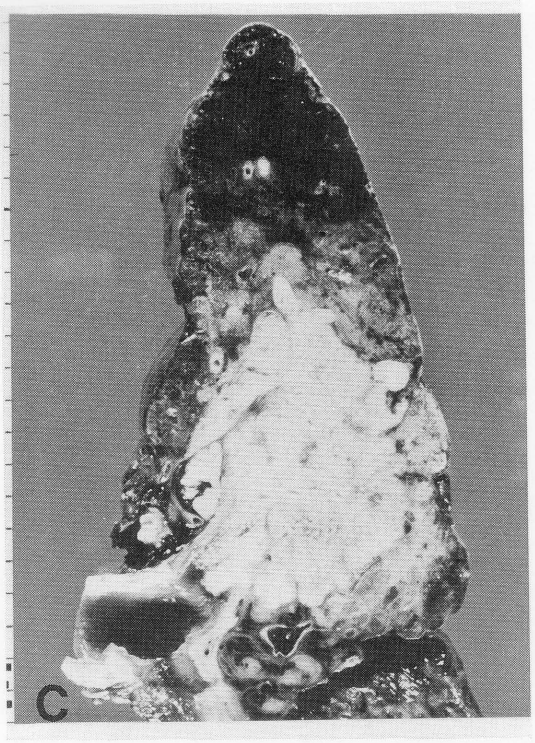


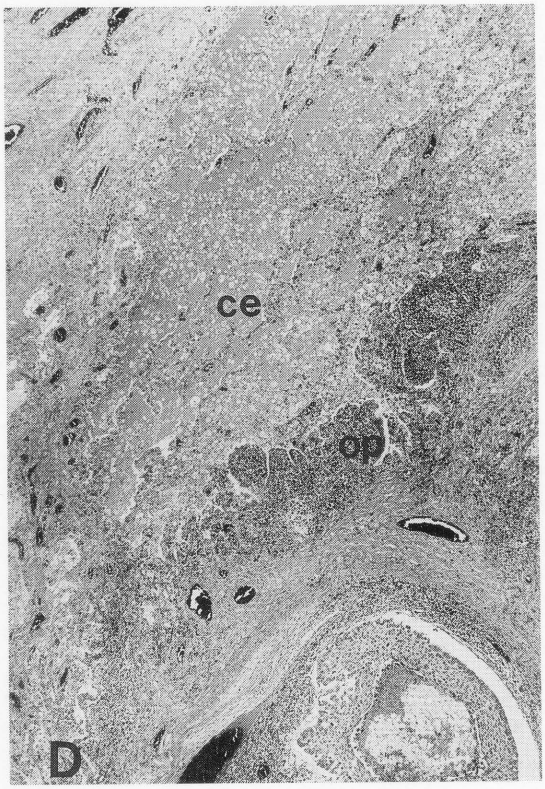


**Fig. 6** A 55-yr-old man with SqCC. The chest radiogram (A) shows collapse of the right upper lobe. The lesion is imaged as a decreased uptake area (open arrow) with an increased uptake area (solid arrow) in the 4-hr $^{123}$I-IMP posterior image (B). The decreased uptake area corresponded to the tumor, $55 \times 35 \times 60$ mm in size, located in the left upper bronchus and the increased uptake area corresponded to obstructive pneumonitis and collapse in the removed specimen (C). The lung lesion distal to the tumor had microscopic features of obstructive pneumonitis (op), congestive edema (ce) (D) and collapse.

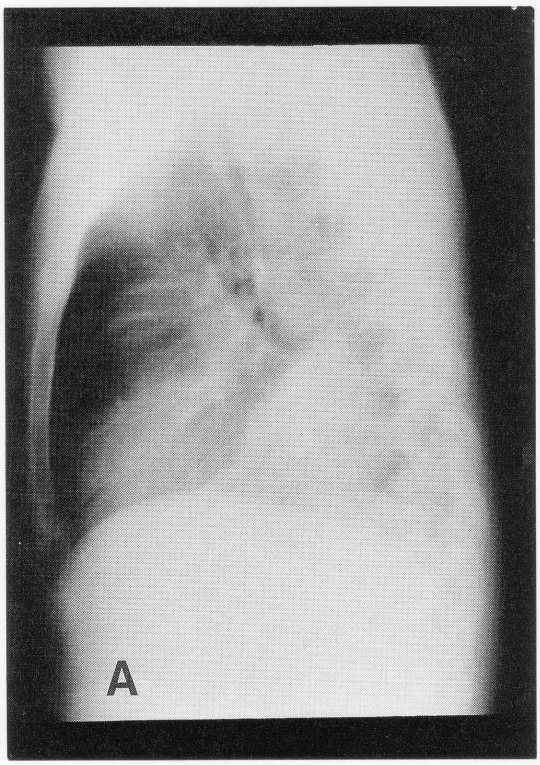


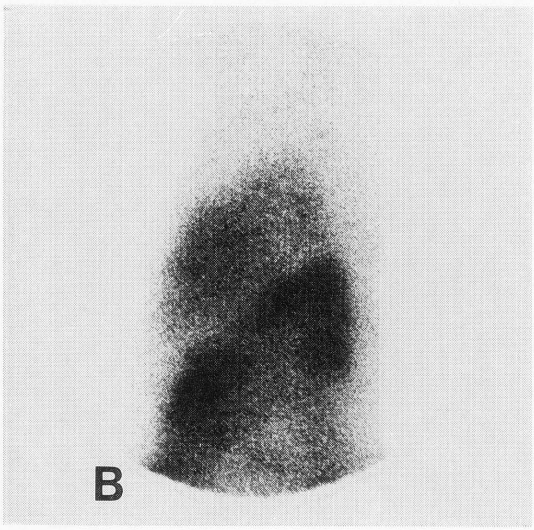

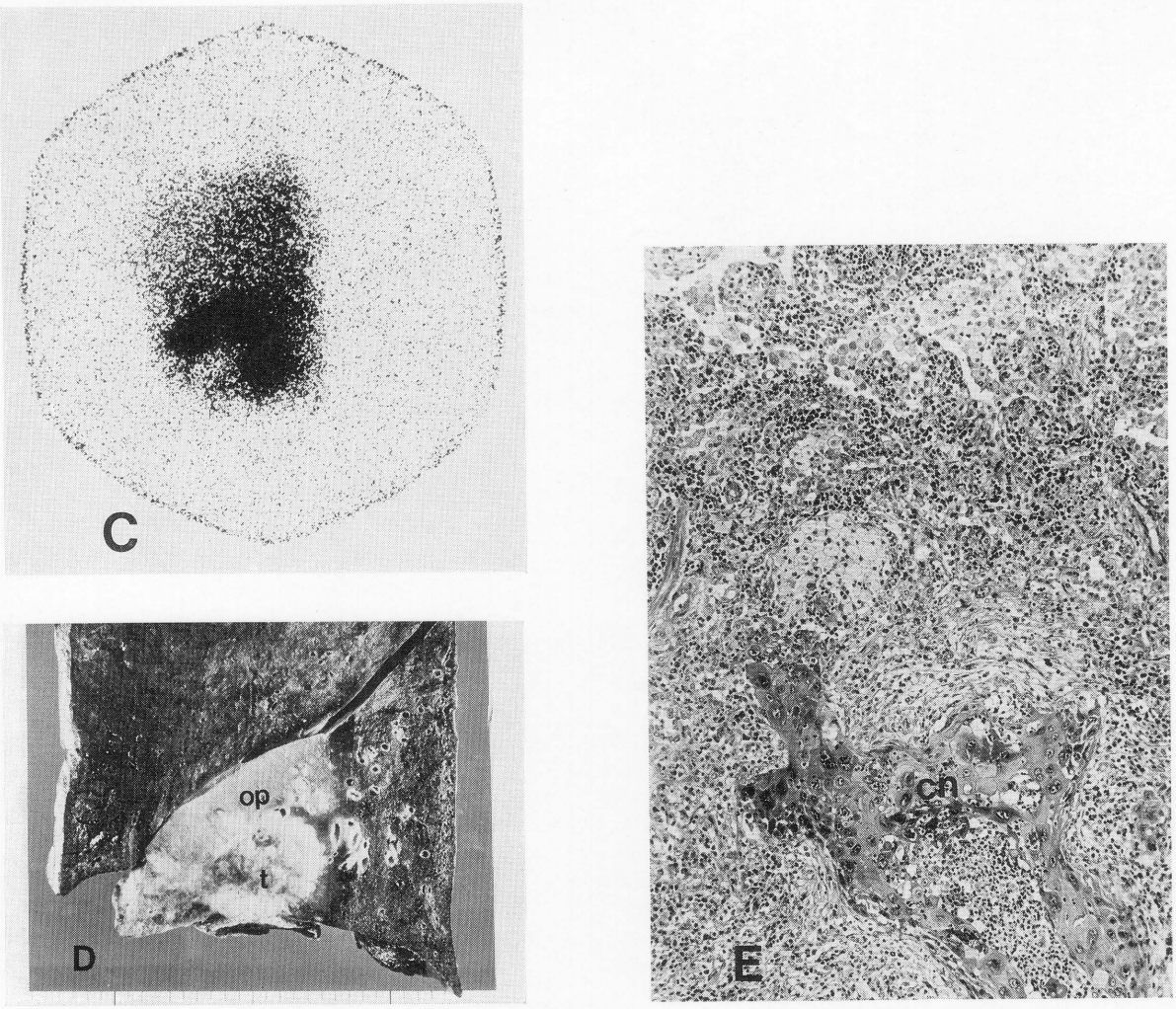


**Fig. 7** A 35-yr-old man with SqCC. A diffuse homogeneous X-ray shadow is present in the left lower lung field (A). The lesion shows a decreased uptake area with an increased uptake area in the 4-hr I-123 IMP left lateral image (B). The 24-hr I-123 IMP left lateral view (C) of the removed left lung is analogous to the 4-hr image (B). The decreased and increased uptake areas are shown to correspond to the tumor (t) and obstructive pneumonitis (op), respectively, in a cross section of the removed specimen (D). The increased uptake lesion had the microscopic features of obstructive pneumonitis surrounding cancer cell nests (cn) (E) and congestive edema.

Since the potential of I-123 IMP for the assessment of lung pathology has been shown,[2] several investigators including us have applied this agent for lung imaging in several types of lung disease.[8–11]

We reported a case of lung cancer in which I-123 IMP did not concentrate in a lung cancer but concentrated in inflammatory lesions surrounding it.[8] This experience also prompted us to further study I-123 IMP lung imaging in patients with bronchogenic carcinoma and preliminary results suggested a difference in uptake of I-123 IMP between cancer itself and secondary changes.[9]

The present study confirmed that I-123 IMP did not accumulate in a bronchogenic carcinoma but accumulated gradually in carcinoma associated secondary changes, such as obstructive pneumonitis or collapse. The mechanism of I-123 IMP accumulation in these secondary changes is not fully understood. An increase in pulmonary arterial blood flow is not the cause because Tc-99m MAA lung perfusion imaging demonstrated decreased perfusion of the lesions in all cases studied. The initial one or 2-min I-123 IMP dynamic lung image also showed decreased activity in the lesions in all cases. A gradual increase in activity in the areas of secondary changes suggests that I-123 IMP or its metabolites such as p-iodoamphetamine[12] may enter the lesion via the pulmonary arteries and/or bronchial arteries during recirculation. The major sites of retention of the activity may be the extravascular spaces such as the

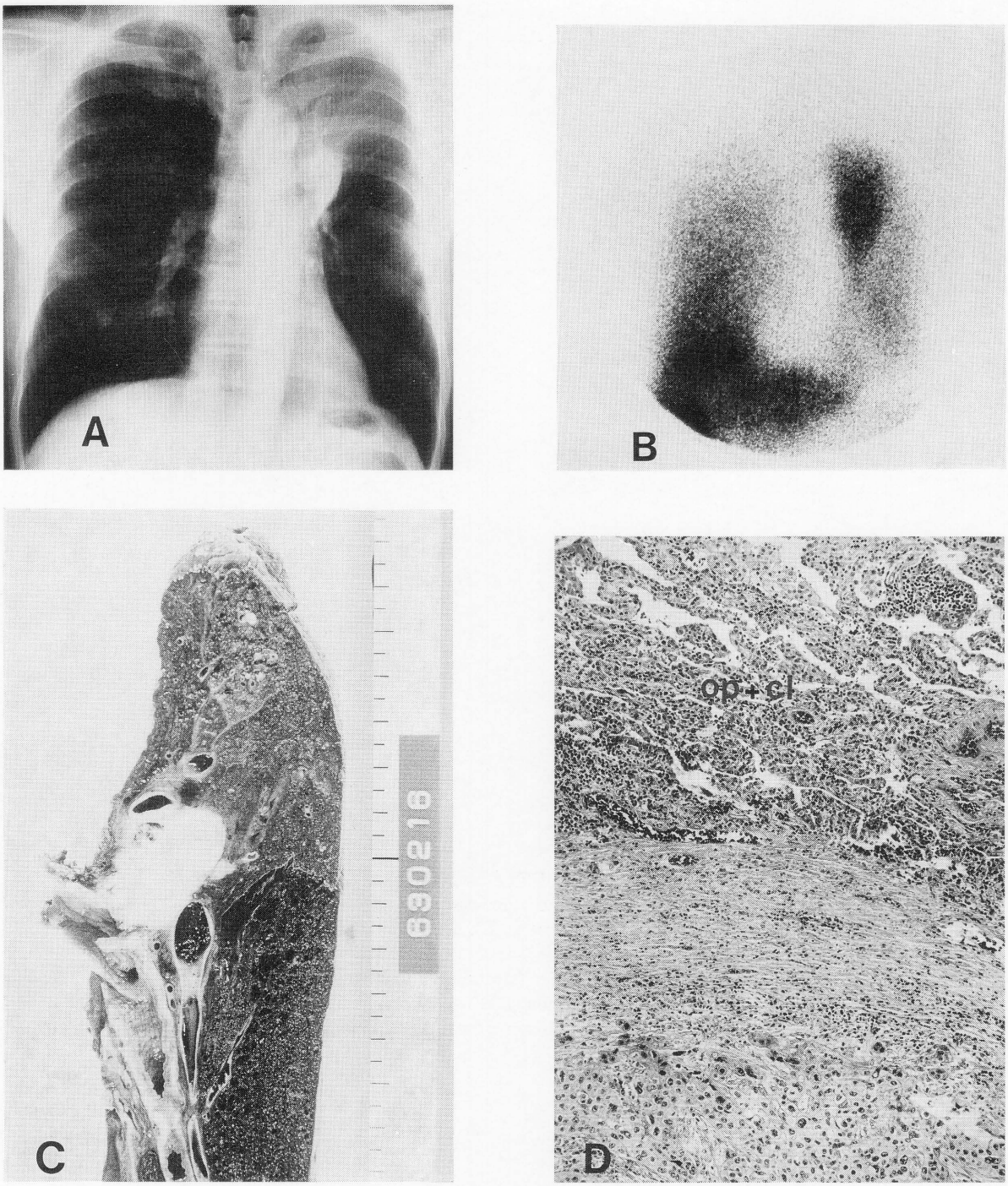


**Fig. 8** A 70-yr-old man with SqCC. A collapse was observed radiographically in the left upper lobe (A). An increased uptake area is seen in the 4-hr I-123 IMP anterior image (B). The tumor was $36 \times 19 \times 30$ mm in size with distal collapse (C). The distal lesion had microscopic features of obstructive pneumonitis (op) and collapse (cl) (D) and had congestive edema.

alveoli and interalveolar septa where inflammatory features were observed pathologically. Increased vascular permeability due to inflammation may permit diffusion of I-123 IMP and/or its metabolite(s) into such extravascular spaces. The activity may be in edema and/or within inflammatory cells such as macrophages. In fact, recent studies showed that the activity from I-123 IMP was much higher in the cellular and/or noncellular components of the bronchoalveolar lavage fluid than in the serum.[13,14] Retention of I-123 IMP and/or its metabolite(s) in such abnormal sites may result in delayed clearance

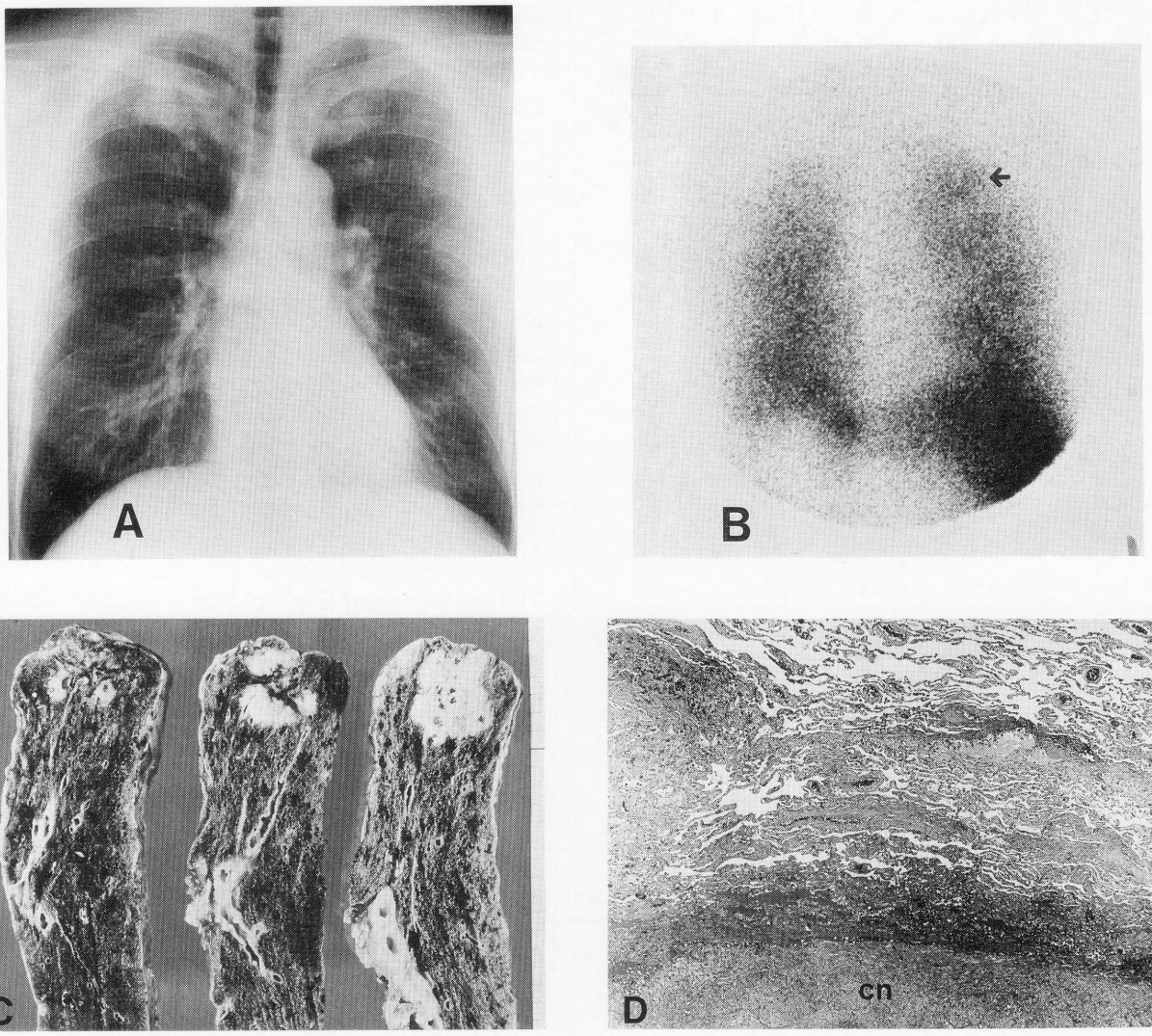


**Fig. 9** A 67-yr-old man with Adenoca. A mass shadow in the right upper lung field (A) corresponded to the increased uptake area (arrow) in the 4-hr I-123 IMP posterior image (B). The removed specimen revealed a tumor, $31 \times 29 \times 30$ mm in size (C) which accompanied congestive edema, obstructive pneumonitis surrounding cancer cell nests (cn) (D) and infarction demonstrated microscopically.

of the activity and thus clear visualization of the lesions at 4 hr. The decreased activity in the tumor may be due to reduced pulmonary arterial blood flow and/or lack of endothelial amine receptors which are believed to be the binding sites for I-123 IMP in normal lungs.[15] Impaired uptake of I-123 IMP has also been noted in brain tumors.[16]

Decreased I-123 IMP uptake was observed in the cavities of lung abscesses, tuberculomas and metastatic lung cancer,[9–11] while in contrast other lesions which showed a gradual increase in I-123 IMP activity were due to bacterial, viral, tuberculous, interstitial and radiation pneumonia or pneumonitis.[9–11] The nodules of pneumoconiosis showed either decreased or increased I-123 IMP uptake.[9]

In this series, a mass shadow could be identified in 53 lesions by radiograms. Only one mass shadow appeared to show a pattern of an increased uptake area. Pathologically, this lesion consisted of a small tumor surrounded by obstructive pneumonitis, congestive edema and infarction. Therefore, the increased activity in the surrounding lesion might have masked the defect of the tumor. Eight other mass shadows with no apparant radiographic changes around the mass showed a rim of increased activity around the tumor. Of these, 3 lesions were removed and had pathological evidence of obstructive pneumonitis surrounding the tumor.

The differentiation of bronchogenic carcinoma from postobstructive lobar collapse is sometimes difficult even when using TCT and magnetic resonance imaging (MRI):[17] The precontrast TCT scan

**Table 3** Chest X-ray findings corresponding to a decreased uptake area (D) and an increased (I) or further increased (FI) area in the 4-hr I-123 IMP images

| Chest X-ray findings | No. of D | No. of I (FI) |
|---|---|---|
| Mass | 52 | 1 |
| Infiltrates | 1 | 32 |
| Infiltrates with consolidation | | 1 |
| Infiltrates with honeycombing | | 2 |
| Collapse | | 16 |
| Honeycombing | | 2 |
| Consolidation | | 1 |
| No apparant change surrounding a mass | | 8 |
| Pleural effusion | 3 | |
| An area of infiltrates, | 3 | |
| collapse | 2 | |
| and diffuse homogeneous shadow | 2 | 2 |
| Total | 63 | 65 |

did not separate proximal tumor from distal lobar collapse by attenuation values. Bolus/drip infusion TCT technique did not differentiate tumor from collapsed lung in either of two cases. Only dynamic scanning with bolus injection performed at a preselected level allowed differentiation by attenuation values in 8 of 10 patients. MRI separated tumor from collapsed lung in 8 of 18 (44%) cases. Concentration of Ga-67 citrate in a wide variety of malignant and benign diseases is well known.[18] Therefore Ga-67 citrate imaging cannot discriminate bronchogenic carcinoma from inflammation.[8]

Although in 14 of 74 lesions, only the secondgry changes were depicted, 4-hr I-123 IMP imaging has the potential to discriminate between bronchogenic carcinoma and secondary changes, such as obstructive pneumonitis or collapse in all cases because of the differences in accumulation of I-123 IMP and/or its metabolites into these two pathological states. The application of single photon emission computed tomography to I-123 IMP lung imaging will depict the relations between tumor and secondary changes in more detail.

From the clinical standpoint, I-123 IMP lung

**Table 4** Comparison of lesion findings in the 4-hr I-123 IMP images and surgically removed specimens in 29 patients with bronchogenic carcinoma

| Histology* | No. of specimens | 4-hr I-123 IMP findings | | Pathological findings | |
|---|---|---|---|---|---|
| | | Findings** | No. of lesions | Findings*** | No. of lesions |
| SqCC | 18 | D | 11 | Tumor | 11 |
| | | I (FI) | 18 | OP | 10 |
| | | | | OP+C | 1 |
| | | | | OP+CE | 1 |
| | | | | OP+BP+CE | 1 |
| | | | | OP+BP+C | 1 |
| | | | | CL+CE | 1 |
| | | | | CL+OP+CE | 3 |
| Adenoca | 8 | D | 7 | Tumor | 7 |
| | | I (FI) | 4 | OP+C | 2 |
| | | | | CL+OP+CE | 1 |
| | | | | Tumor+OP+CE +IF | 1 |
| | | N | 4 | NS | 4 |
| SCLC | 1 | I | 1 | OP+CE | 1 |
| BAC | 2 | D | 2 | Tumor | 2 |
| | | I | 1 | IP | 1 |

*,** Abbreviations are the same as used in Table 1.

*** Abbreviations are as follows: OP; obstructive pneumonitis, C; congestion, CE; congestive edema, BP; bronchopneumonia, CL; collapse, IF; infarction, NS; no significant change, IP; interstitial pneumonia with epitheloid cell granuloma.

imaging will be indicated in suspected bronchogenic carcinoma, when (a) X-ray and/or TCT examinations cannot discriminate the extent of the tumor from the secondary change, (b) a large atelectatic or homogeneous shadow or total opacity of the unilateral lung is observed in the chest X-ray films, (c) there is an unusual shadow for lung cancer, e.g., infiltrates in BAC and (d) other diagnostic methods fail to differentiate cancer from a benign disease. In these situations, I-123 IMP lung imaging will provide useful diagnostic information by depicting normal and pathological lung tissues as having different degrees of the activity.


## ACKNOWLEDGMENT

The authors thank Prof. B. Shapiro (The University of Michigan Medical Center, Ann Arbor) for correcting the English text.


## REFERENCES


1. Winchell HS, Baldwin RM, Lin TH: Development of I-123-labeled amines for brain studies: localization of I-123 iodophenylalkyl amines in rat brain. *J Nucl Med* 21: 940–946, 1980
2. Touya J, Akber SF, Rahimian J, et al: Metabolic lung scanning with N-isopropyl-I-123-iodoamphetamine. In: Raynaud C, ed. Proceedings of the Third World Congress of Nuclear Medicine and Biology. Paris: Pergamon Press, 2554–2557, 1982
3. Hill TC, Holman BL, Lovett R, et al: Initial experience with SPECT (single-photon emission computerized tomography) of the brain using N-isopropyl I-123 p-iodoamphetamine: Concise communication. *J Nucl Med* 23: 191–195, 1982
4. Holman BL, Hill TC, Polak JF, et al: Cerebral perfusion imaging with iodine 123-labeled amines. *Arch Neurol* 41: 1060–1063, 1984
5. Coni NK, Wraight EP, Barber RW: Regional cerebral perfusion imaging in the elderly. *Age and Aging* 13: 214–217, 1984
6. Gemmell HG, Sharp PF, Evans NTS, et al: Single photon emission tomography with $^{123}$I-isopropyl-amphetamine in Alzheimer's disease and multinfarct dementia. *Lancet* 2: 1348, 1984
7. Magistretti P, Uren R, Blume H, et al: Delineation of epileptic focus by single photon emission tomography. *Eur J Nucl Med* 7: 484–485, 1982
8. Nakajo M, Uchiyama N, Hiraki Y, et al: Increased accumulation of iodine-123 IMP in the pulmonary inflammatory lesion surrounding a lung cancer. *Ann Nucl Med* 2: 49–53, 1988
9. Nakajo M, Shimada J, Shimozono M, et al: Serial lung imaging with $^{123}$I-IMP in localized pulmonary lesions. *Jpn J Nucl Med* 25: 441–450, 1988
10. Suga K, Matsumoto T, Nakanishi T, et al: Clinical study on the mechanism of abnormal accumulation in lung scanning with N-isopropyl-p-$^{123}$I-iodoamphetamine ($^{123}$I-IMP). *Jpn J Nucl Med* 25: 625–631, 1988
11. Suematsu T, Narabayashi I, Takada Y, et al: Delayed lung scintigraphy with N-isopropyl-I-123-p-iodoamphetamine in lung cancer and inflammatory disease. *Jpn J Nucl Med* 26: 45–53, 1989
12. Baldwin RM, Wu J-L: In vivo chemistry of iofetamine HCl iodine-123 (IMP). *J Nucl Med* 29: 122–124, 1988
13. Itasaka M, Ikeda H, Yakuma N, et al: The study of the lung accumulation of I-123 IMP by the bronchoalveolar lavage. *Jpn J Nucl Med* 26: 189–194, 1989
14. Kosuda S, Kawahara S, Tamura K, et al: Evaluation of the lung uptake of $^{123}$I-IMP by bronchoalveolar lavage. *Nippon Act Radiol* 49: 484–486, 1989
15. Rahimian J, Glass EC, Touya JJ, et al: Measurement of metabolic extraction of tracers in the lung using a multiple indicator dilution technique. *J Nucl Med* 25: 31–37, 1984
16. Lafrance ND, Wagner HN, Whitehouse P, et al: Decreased accumulation of isopropyl-iodoamphetamine (I-123) in brain tumors. *J Nucl Med* 22: 1081–1083, 1981
17. Tobler J, Levitt RG, Glazer HS, et al: Differentiation of proximal bronchogenic carcinoma from postobstructive lobar collapse by magnetic resonance imaging comparison with computed tomography. *Invest Radiol* 22: 538–543, 1987
18. Larson SM, Camargo EE, Keenan AM: Tumors. Textbook of Nuclear Medicine, Vol. 2: Clinical application, Harbest J, da Rocha AFG, eds. Philadelphia, Lea & Febiger, pp 635–662, 1984